

# STRIPE FLUCTUATIONS, CARRIERS, SPECTROSCOPIES, TRANSPORT, AND BCS–BEC CROSSOVER IN THE HIGH- $T_c$ CUPRATES

J. ASHKENAZI

Physics Department, University of Miami, P.O. Box 248046, Coral Gables, FL 33124, U.S.A.

**Abstract**—The quasiparticles of the high- $T_c$  cuprates are found to consist of: polaron-like “stripions” carrying charge, and associated primarily with large- $U$  orbitals in stripe-like inhomogeneities; “quasi-electrons” carrying charge and spin, and associated with hybridized small- $U$  and large- $U$  orbitals; and “svivons” carrying spin and lattice distortion. It is shown that this electronic structure leads to the systematic behavior of spectroscopic and transport properties of the cuprates. High- $T_c$  pairing results from transitions between pair states of stripions and quasi-electrons through the exchange of svivons. The cuprates fall in the regime of crossover between BCS and preformed-pairs Bose-Einstein condensation behaviors.

First-principles calculations in the cuprates support an approach based on the existence of both “large- $U$ ” and “small- $U$ ” orbitals in the vicinity of the Fermi level ( $E_F$ ). Let us denote the fermion creation operator of a small- $U$  electron in band  $\nu$ , spin  $\sigma$  (which can be assigned a number  $\pm 1$ ), and wave vector  $\mathbf{k}$  by  $c_{\nu\sigma}^\dagger(\mathbf{k})$ . The large- $U$  orbitals in the  $\text{CuO}_2$  planes are approached through the “slave-fermion” method [1]. A large- $U$  electron in site  $i$  and spin  $\sigma$  is then created by  $d_{i\sigma}^\dagger = e_i^\dagger s_{i,-\sigma}$ , if it is in the “upper-Hubbard-band”, and by  $d_{i\sigma}^\dagger = \sigma s_{i\sigma}^\dagger h_i$ , if it is in a Zhang-Rice-type “lower-Hubbard-band”. Here  $e_i$  and  $h_i$  are (“excession” and “holon”) fermion operators, and  $s_{i\sigma}$  are (“spinon”) boson operators. These auxiliary particles have to satisfy the constraint:  $e_i^\dagger e_i + h_i^\dagger h_i + \sum_\sigma s_{i\sigma}^\dagger s_{i\sigma} = 1$ .

Within the “auxiliary space” a chemical-potential-like Lagrange multiplier is introduced to impose the constraint on the average. Physical observables are calculated as combinations of Green’s functions of the auxiliary space. Since the time evolution of Green’s functions is determined by the Hamiltonian which obeys the constraint rigorously, it is not expected to be violated as long as the approximations used for these Green’s functions are justifiable.

The spinon states are diagonalized by applying the Bogoliubov transformation [2]:

$$s_\sigma(\mathbf{k}) = \cosh(\xi_{\mathbf{k}})\zeta_\sigma(\mathbf{k}) + \sinh(\xi_{\mathbf{k}})\zeta_{-\sigma}^\dagger(-\mathbf{k}). \quad (1)$$

The Bose operators  $\zeta_\sigma^\dagger(\mathbf{k})$  create spinon states of “bare” energies  $\epsilon^\zeta(\mathbf{k})$  which have a V-shape zero minimum at  $\mathbf{k} = \mathbf{k}_0$ . Bose condensation results in antiferromagnetic (AF) order at wave vector

$\mathbf{Q} = 2\mathbf{k}_0$ . The values of  $\mathbf{k}$  are within a Brillouin zone (BZ) determined by adding  $\mathbf{Q}$  to the basic reciprocal lattice. For  $\mathbf{k} \rightarrow \mathbf{k}_0$  one has [2]  $\cosh(\xi_{\mathbf{k}}) \cong -\sinh(\xi_{\mathbf{k}}) \gg 1$ .

Theoretical calculations [3] predict that a lightly doped AF plane tends to form a frustrated striped structure where narrow charged stripes form antiphase domain walls separating wider AF stripes. Various experiments [4] (including EXAFS, magnetic neutron scattering, channeling, inelastic neutron scattering, NQR, NMR, ARPES, PDF, heat transport, phonon screening, *etc*) support the idea that the high- $T_c$  cuprates are characterized by such a fluctuating striped structure. Within the one dimensional charged stripes the spin-charge separation approximation is expected to be valid. Under this approximation two-particle spinon-holon (spinon-excession) Green’s functions are decoupled into single-auxiliary-particle Green’s functions, and auxiliary particles can be interpreted as physical quasiparticles.

Holons (excessions) within the charged stripes are referred to as “stripions”. Their creation operators (creating charge  $-e$ ) are denoted by  $p_\mu^\dagger(\mathbf{k})$ , and bare energies by  $\epsilon_\mu^p(\mathbf{k})$ . Since these dynamical stripes are highly inhomogeneous and segmented, we find it more appropriate to assume a starting point of localized, rather than itinerant, stripion states. The  $\mathbf{k}$  quantum number here presents a  $\mathbf{k}$ -symmetrized combination of degenerate localized states to be treated in a perturbation expansion. These values of  $\mathbf{k}$  are within a BZ based on periodic supercells which are large enough to approximately contain (each) the entire spectrum  $\epsilon_\mu^p$  of bare stripion energies. These supercells introduce an approximate

long-range order in spite of the local inhomogeneity introduced by the dynamical striped structure.

Holons (excessions) away from the charged stripes are not decoupled from the spinons. One can construct within the auxiliary space approximate fermion creation operators of coupled holon-spinon (excession-spinon) basis states as follows:

$$f_{\lambda\sigma}^\dagger(\mathbf{k}', \mathbf{k}) = \frac{e_\lambda^\dagger(\mathbf{k}')s_{\lambda,-\sigma}(\mathbf{k}' - \mathbf{k})}{\sqrt{n_\lambda^e(\mathbf{k}') + n_{\lambda,-\sigma}^s(\mathbf{k}' - \mathbf{k})}}, \quad (2)$$

$$g_{\lambda\sigma}^\dagger(\mathbf{k}', \mathbf{k}) = \frac{\sigma h_\lambda(\mathbf{k}')s_{\lambda\sigma}^\dagger(\mathbf{k} - \mathbf{k}')}{\sqrt{n_\lambda^h(\mathbf{k}') + n_{\lambda\sigma}^s(\mathbf{k} - \mathbf{k}')}}, \quad (3)$$

where these values of  $\mathbf{k}$  are within the BZ of the basic lattice. An index  $\lambda$  has been introduced to account for the effect of more than one  $\text{CuO}_2$  layer within the unit cell, and:  $n_\lambda^e(\mathbf{k}) \equiv \langle e_\lambda^\dagger(\mathbf{k})e_\lambda(\mathbf{k}) \rangle$ ,  $n_\lambda^h(\mathbf{k}) \equiv \langle h_\lambda^\dagger(\mathbf{k})h_\lambda(\mathbf{k}) \rangle$ ,  $n_{\lambda\sigma}^s(\mathbf{k}) \equiv \langle s_{\lambda\sigma}^\dagger(\mathbf{k})s_{\lambda\sigma}(\mathbf{k}) \rangle$ .

The mean-field eigenstates of the Hamiltonian, obtained within the auxiliary space as combinations of the above basis states (more rigorously, these states have to be orthogonalized to the stripon states, and depleted), and the small- $U$  states [created by  $c_{i\sigma}^\dagger(\mathbf{k})$ ] are referred to as ‘‘quasi-electron’’ (QE) states. Their creation operators are denoted by  $q_{i\sigma}^\dagger(\mathbf{k})$ , and bare energies by  $\epsilon_i^q(\mathbf{k})$ . These energies form quasi-continuous ranges of bands within the BZ, and part of them cross  $E_F$ . The QE states close to  $E_F$  introduce fluctuations to the AF stripes, but do not destroy the AF correlations.

The QE, stripon and spinon fields are strongly coupled to each other due to hopping and hybridization terms of the Hamiltonian. This coupling can be expressed through an effective Hamiltonian term whose parameters can be in principle derived self-consistently from the original Hamiltonian. Discussing, *e.g.*, the case of p-type cuprates, the coupling Hamiltonian has the form:

$$\begin{aligned} \mathcal{H}' = & \frac{1}{\sqrt{N}} \sum_{i\lambda\mu\sigma} \sum_{\mathbf{k}, \mathbf{k}'} \{ \sigma \epsilon_{i\lambda\mu}^{qp}(\mathbf{k}, \mathbf{k}') q_{i\sigma}^\dagger(\mathbf{k}) p_\mu(\mathbf{k}') \\ & \times [\cosh(\xi_{\lambda, \mathbf{k}-\mathbf{k}'}) \zeta_{\lambda\sigma}(\mathbf{k} - \mathbf{k}') \\ & + \sinh(\xi_{\lambda, \mathbf{k}-\mathbf{k}'}) \zeta_{\lambda,-\sigma}^\dagger(\mathbf{k}' - \mathbf{k})] + h.c. \}, \quad (4) \end{aligned}$$

where the  $\mathbf{k}$  values correspond to the supercell stripons BZ, within which the other fields have been embedded, multiplying the number of their bands, and redefining their band indices appropriately. Thus  $\mathcal{H}'$  introduces a vertex between the QE, stripon and spinon propagators [5].

As was observed [6] a localized stripon modifies the lattice in its vicinity. Thus, any physical process induced by  $\mathcal{H}'$ , where a stripon is transformed

into a QE, or vice versa, and a spinon is emitted and/or absorbed, necessarily involves also the emission and/or absorption of phonons. This can be formulated by multiplying a spinon propagator, linked to the  $\mathcal{H}'$  vertex with a power series of phonon propagators [5]. We refer to such a phonon-‘‘dressed’’ spinon as a ‘‘svivon’’; it carries spin and lattice distortion. The  $\mathcal{H}'$  vertex is now interpreted as coupling between a QE, stripon, and svivon propagators.

The electrons spectral function at momentum  $\mathbf{p}$  and energy  $\omega$ ,  $A_e(\mathbf{p}, \omega) \equiv \Im \mathcal{G}_e(\mathbf{p}, \omega - i0^+)/\pi$  (where  $\mathcal{G}_e$  is the electrons Green’s function) is expressed in terms of auxiliary space spectral functions  $A_i^q(\mathbf{k}, \omega)$ ,  $A_\mu^p(\mathbf{k}, \omega)$ , and  $A_\lambda^\zeta(\mathbf{k}, \omega)$  of the QE’s, stripsons, and svivons, respectively. It will be shown below that the resulting stripon bandwidth is much smaller than the QE and svivon bandwidths. Thus, the same phase-space argument as in the Migdal theorem can be applied to conclude that vertex corrections to the  $\mathcal{H}'$  vertex are negligible. Consequently, a second-order perturbation expansion in  $\mathcal{H}'$  is applicable calculating self-energy correction (see the diagrams in Ref. [5]). The following expressions are obtained for the QE, stripon, and svivon scattering rates  $\Gamma^q(\mathbf{k}, \omega)$ ,  $\Gamma^p(\mathbf{k}, \omega)$ , and  $\Gamma^\zeta(\mathbf{k}, \omega)$  [ $\Gamma(\mathbf{k}, \omega) \equiv 2\Im\Sigma(\mathbf{k}, \omega - i0^+)$ ]:

$$\begin{aligned} \Gamma_{\nu\nu'}^q(\mathbf{k}, \omega) \cong & \frac{2\pi}{N} \sum_{\lambda\mu\mathbf{k}'} \int d\omega' \epsilon_{i\lambda\mu}^{qp}(\mathbf{k}', \mathbf{k}) \epsilon_{i'\lambda\mu}^{qp}(\mathbf{k}', \mathbf{k})^* \\ & \times A_\mu^p(\mathbf{k}', \omega') [-\cosh^2(\xi_{\lambda, \mathbf{k}-\mathbf{k}'}) A_\lambda^\zeta(\mathbf{k} - \mathbf{k}', \omega - \omega') \\ & + \sinh^2(\xi_{\lambda, \mathbf{k}-\mathbf{k}'}) A_\lambda^\zeta(\mathbf{k} - \mathbf{k}', \omega' - \omega)] \\ & \times [f_T(\omega') + b_T(\omega' - \omega)], \quad (5) \end{aligned}$$

$$\begin{aligned} \Gamma_{\mu\mu'}^p(\mathbf{k}, \omega) \cong & \frac{2\pi}{N} \sum_{i\mathbf{k}'\sigma} \int d\omega' \epsilon_{i\lambda\mu}^{qp}(\mathbf{k}', \mathbf{k})^* \epsilon_{i'\lambda\mu'}^{qp}(\mathbf{k}', \mathbf{k}) \\ & \times A_i^q(\mathbf{k}', \omega') [\cosh^2(\xi_{\lambda, \mathbf{k}'-\mathbf{k}}) A_\lambda^\zeta(\mathbf{k}' - \mathbf{k}, \omega' - \omega) \\ & - \sinh^2(\xi_{\lambda, \mathbf{k}'-\mathbf{k}}) A_\lambda^\zeta(\mathbf{k}' - \mathbf{k}, \omega - \omega')] \\ & \times [f_T(\omega') + b_T(\omega' - \omega)], \quad (6) \end{aligned}$$

$$\begin{aligned} \Gamma_{\lambda\lambda'}^\zeta(\mathbf{k}, \omega) \cong & \frac{2\pi}{N} \sum_{i\mathbf{k}'\mu} \int d\omega' \epsilon_{i\lambda\mu}^{qp}(\mathbf{k}', \mathbf{k}' - \mathbf{k})^* \\ & \times \epsilon_{i'\lambda'\mu}^{qp}(\mathbf{k}', \mathbf{k}' - \mathbf{k}) [\cosh(\xi_{\lambda\mathbf{k}}) \cosh(\xi_{\lambda'\mathbf{k}}) A_i^q(\mathbf{k}', \omega') \\ & \times A_\mu^p(\mathbf{k}' - \mathbf{k}, \omega' - \omega) + \sinh(\xi_{\lambda\mathbf{k}}) \sinh(\xi_{\lambda'\mathbf{k}}) \\ & \times A_i^q(\mathbf{k}', -\omega') A_\mu^p(\mathbf{k}' - \mathbf{k}, \omega - \omega')] \\ & \times [f_T(\omega' - \omega) - f_T(\omega')], \quad (7) \end{aligned}$$

where  $f_T(\omega)$  and  $b_T(\omega)$  are the Fermi and Bose distribution functions at temperature  $T$ .

The real parts of the self energies and the spectral functions are obtained through the relations:

$$\Re\Sigma(\mathbf{k}, \omega) = \wp \int \frac{d\omega' \Gamma(\mathbf{k}, \omega')}{2\pi(\omega - \omega')}, \quad (8)$$

$$A(\mathbf{k}, \omega) = \frac{\Gamma(\mathbf{k}, \omega)/2\pi}{[\omega - \epsilon(\mathbf{k}) - \Re\Sigma(\mathbf{k}, \omega)]^2 + [\Gamma(\mathbf{k}, \omega)/2]^2}. \quad (9)$$

Matrix diagonalization is necessary to determine the poles of the Green's functions, however only the diagonal terms are needed to determine the spectral functions.

For sufficiently doped cuprates a self-consistent solution is obtained with three energy ranges. Expressions are derived below for the intermediary energy range. The high energy range, above few tenths of an eV (determined by the exchange energies of the large- $U$  spins) is treated by introducing cut-off integration limits at  $\pm\omega_c$  to the Eq. (8) integrals, resulting in spurious logarithmic divergences at  $\pm\omega_c$ . The low energy range, below  $\sim 0.02$  eV, introduces a “zero-energy” non-analytic behavior to these expressions (analyticity is restored within the low-energy range).

For simplicity, the dependencies of the functions and the coefficients on  $\mathbf{k}$  and the band indices is omitted in these expressions. All the coefficients are positive. Variation of the matrix elements in Eqs. (5–7) is ignored, and sums of the quasiparticle spectral functions over the band indices and small  $\mathbf{k}'$  ranges are expressed as:

$$\tilde{A}^q(\omega) \cong \begin{cases} a_+^q \omega + b_+^q, & \text{for } \omega > 0, \\ -a_-^q \omega + b_-^q, & \text{for } \omega < 0, \end{cases} \quad (10)$$

$$\tilde{A}^p(\omega) \cong \delta(\omega), \quad (11)$$

$$\tilde{A}^\zeta(\omega) \cong \begin{cases} a_+^\zeta \omega + b_+^\zeta, & \text{for } \omega > 0, \\ a_-^\zeta \omega - b_-^\zeta, & \text{for } \omega < 0. \end{cases} \quad (12)$$

These expressions will be derived below self-consistently. By Inserting them in Eqs. (5–7), expressions of the following forms are derived, assuming the low  $T$  limits for  $f_T(\omega)$  and  $b_T(\omega)$ :

$$\frac{\Gamma^q(\omega)}{2\pi} \cong \begin{cases} c_+^q \omega + d_+^q, & \text{for } \omega > 0, \\ -c_-^q \omega + d_-^q, & \text{for } \omega < 0, \end{cases} \quad (13)$$

$$\frac{\Gamma^p(\omega)}{2\pi} \cong \begin{cases} c_+^p \omega^3 + d_+^p \omega^2 + e_+^p \omega, & \text{for } \omega > 0, \\ -c_-^p \omega^3 + d_-^p \omega^2 - e_-^p \omega, & \text{for } \omega < 0, \end{cases} \quad (14)$$

$$\frac{\Gamma^\zeta(\omega)}{2\pi} \cong \begin{cases} c_+^\zeta \omega + d_+^\zeta, & \text{for } \omega > 0, \\ c_-^\zeta \omega - d_-^\zeta, & \text{for } \omega < 0. \end{cases} \quad (15)$$

Integrating through Eq. (8) (between the limits  $\pm\omega_c$ ) results in:

$$\begin{aligned} -\Re\Sigma^q(\omega) \cong & \omega_c(c_+^q - c_-^q) + (d_+^q \ln \left| \frac{\omega - \omega_c}{\omega} \right| \\ & - d_-^q \ln \left| \frac{\omega + \omega_c}{\omega} \right|) + \omega(c_+^q \ln \left| \frac{\omega - \omega_c}{\omega} \right| \end{aligned}$$

$$+ c_-^q \ln \left| \frac{\omega + \omega_c}{\omega} \right|), \quad (16)$$

$$\begin{aligned} -\Re\Sigma^p(\omega) \cong & \left[ \frac{\omega_c^3}{3}(c_+^p - c_-^p) + \frac{\omega_c^2}{2}(d_+^p - d_-^p) \right. \\ & + \omega_c(e_+^p - e_-^p)] + \omega \left[ \frac{\omega_c^2}{2}(c_+^p + c_-^p) \right. \\ & + \omega_c(d_+^p + d_-^p) + e_+^p \ln \left| \frac{\omega - \omega_c}{\omega} \right| \\ & + e_-^p \ln \left| \frac{\omega + \omega_c}{\omega} \right|] + \omega^2[\omega_c(c_+^p - c_-^p) \\ & + d_+^p \ln \left| \frac{\omega - \omega_c}{\omega} \right| - d_-^p \ln \left| \frac{\omega + \omega_c}{\omega} \right|] \\ & + \omega^3[c_+^p \ln \left| \frac{\omega - \omega_c}{\omega} \right| + c_-^p \ln \left| \frac{\omega + \omega_c}{\omega} \right|], \quad (17) \end{aligned}$$

$$\begin{aligned} -\Re\Sigma^\zeta(\omega) \cong & \omega_c(c_+^\zeta + c_-^\zeta) + (d_+^\zeta \ln \left| \frac{\omega - \omega_c}{\omega} \right| \\ & + d_-^\zeta \ln \left| \frac{\omega + \omega_c}{\omega} \right|) + \omega(c_+^\zeta \ln \left| \frac{\omega - \omega_c}{\omega} \right| \\ & - c_-^\zeta \ln \left| \frac{\omega + \omega_c}{\omega} \right|). \quad (18) \end{aligned}$$

The renormalized quasiparticle energies  $\bar{\epsilon} = \epsilon + \Re\Sigma(\bar{\epsilon})$  are obtained by finding the  $\omega$  values for which  $\Re\Sigma(\omega) = \omega - \epsilon$ . Thus the renormalization effect of energies well below  $\omega_c$  is determined by the slope of the  $\Re\Sigma(\omega)$  vs  $\omega$  curves close to  $\omega = 0$ .

The renormalization effect is particularly strong on the stripon energies. It is contributed by a combined effect of the quasi-continuum of QE bands within the auxiliary space. This strong effect is reflected in a significant  $\omega^3$  term in  $\Gamma^p(\omega)$ . Consequently, the stripon bandwidth drops down to the low energy range, and a  $\delta$ -function is appropriate for  $\tilde{A}^p(\omega)$  (11). The expressions for  $\tilde{A}^q(\omega)$  (10) and  $\tilde{A}^\zeta(\omega)$  (12) are obtained by considering the effects of bands crossing zero energy, which, approximately, contribute constant terms due to the normalization of the spectral functions (9), and of higher energy bands, whose contributions are approximately  $\propto \Gamma(\omega)$  (9), or  $\propto \omega$ .

The inequality between the coefficients for positive and negative  $\omega$  in Eqs. (10–15) results mainly because the svivon spectrum is primarily on the  $\omega > 0$  side [ $\int A_\lambda^\zeta(\mathbf{k}, \omega) d\omega = 1$ ], and the inequality  $\cosh^2(\xi_{\mathbf{k}}) > \sinh^2(\xi_{\mathbf{k}})$  of the factors appearing in Eqs. (5–7). For the discussed case of p-type cuprates the following inequalities are built up self-consistently:

$$a_+^q > a_-^q, \quad b_+^q > b_-^q, \quad c_+^q > c_-^q, \quad d_+^q > d_-^q, \quad (19)$$

$$a_+^\zeta > a_-^\zeta, \quad b_+^\zeta > b_-^\zeta, \quad c_+^\zeta > c_-^\zeta, \quad d_+^\zeta > d_-^\zeta. \quad (20)$$

Note, however, that for “real” n-type cuprates (namely, ones where the stripions are based on excess and not holon states) the roles of  $\cosh(\xi_{\mathbf{k}})$  and

$\sinh(\xi_{\mathbf{k}})$  are reversed in  $\mathcal{H}'$  (4), and the expressions derived from it, and consequently the direction of the inequalities is reversed for the QE coefficients (19), but stays the same for the svivon coefficients (20). Also there could be deviations from (19–20) at specific  $\mathbf{k}$  points, and the inequalities almost disappear for svivons close to point  $\mathbf{k}_0$ .

The spectral functions in Eqs. (10–12) are within the auxiliary space, while in order to calculate the physical electrons spectral functions  $A_e(\mathbf{p}, \omega)$ , or related physical properties, their projection into the “physical space” is required. Spectroscopies, like ARPES, measuring the effect of transfer of electrons into, or out of, the crystal do not detect the low-energy signature of the stripon spectral functions, because they are smeared over few tenths of an eV through convolution with svivon spectral functions. Thus they contribute to  $A_e(\mathbf{p}, \omega)$  part of its “incoherent” background. On the other hand, transport properties, discussed below, measure the electrons *within* the crystal, and can detect the stripon energy scale.

The contribution of the QE spectral functions to  $A_e(\mathbf{p}, \omega)$  depends on the expansion coefficients (eigenvectors) of these states in terms of their basis states [created by (2,3)  $f_{\lambda\sigma}^\dagger(\mathbf{k}', \mathbf{k})$ ,  $g_{\lambda\sigma}^\dagger(\mathbf{k}', \mathbf{k})$ , and  $c_{\nu\sigma}^\dagger(\mathbf{k})$ ]. These eigenvectors have quite random phases for almost all the QE states within their quasi-continuum, and thus contribute to  $A_e(\mathbf{p}, \omega)$  another part of its incoherent background. However, few QE states for which the eigenvectors closely correspond to those of real electron bands, contribute “coherent”  $\bar{\epsilon}^q(\mathbf{k})$  bands to  $A_e(\mathbf{p}, \omega)$ . The occupation factors  $n_\lambda^e$ ,  $n_\lambda^h$ , and  $n_\lambda^s$ , appearing in Eqs. (2,3) are reflected in the observed dependence of  $A_e(\mathbf{p}, \omega)$  in correlated electrons systems on such occupation factors [7].

The  $\omega$  dependencies (10–20) derived in the auxiliary space remain valid in the physical space, both for the coherent bands, and for the incoherent background, detected, *e.g.*, in ARPES results. The present results for  $\Gamma^q$  (13) are reflected in the observed non-Fermi-liquid bandwidths, having a  $\propto \omega$  and a constant term. The results for  $\Re\Sigma^q$  (16) are reflected in band slopes which are smaller than the LDA predictions. Also the fact that the QE field is coupled to the stripon and svivon fields within a BZ corresponding to their (lower) periodicities is experimentally reflected in “shadow bands” and further features associated with a superstructure.

There is a peculiar consequence to the logarithmic singularity in  $\Re\Sigma^q$  at  $\omega = 0$ , due to the  $(d_+^q - d_-^q) \ln|\omega|$  term in Eq. (16). For p-type cuprates (19) the consequence of this singularity is that as an  $\bar{\epsilon}^q(\mathbf{k})$  band is getting close to  $E_F$  from

below it is becoming flatter (though it does not narrow accordingly) while from above it becomes steeper, and may pass through an infinite slope resulting in an S-shape triply valued band (this causes smearing of the spectral weight, and blurring the band; note, however, that the effect of the singularity is truncated and smoothed on an energy scale  $\lesssim 0.02$  eV). For “real” n-type cuprates these behaviors below and above  $E_F$  are switched. ARPES data reflects the behavior below  $E_F$ , and results of such band-flattening have been reported in p-type cuprates (recently such an effect has been attributed to electron coupling with phonons [8] or with the resonance mode observed in neutron scattering [9]; also the observed renormalization of van Hove singularities to extended ones may reflect this effect). The behavior above  $E_F$  would be detected in ARPES measurements. Careful measurements of the bands of n-type cuprates very close to  $E_F$  would help determine whether they are “real” n-type ones.

$\Re\Sigma^\zeta(\omega)$  (18) is negative in the intermediary energy range, and its  $\omega$  dependence is weak, except for the vicinity of  $\omega = 0$ , where a negative logarithmic singularity exists, due to the  $(d_+^\zeta + d_-^\zeta) \ln|\omega|$  term in Eq. (18), turning into a smooth minimum in the low energy range. Consequently, the svivon quasi-particle energies are renormalized through a negative energy shift, resulting in negative  $\bar{\epsilon}^\zeta(\mathbf{k})$  values close to their minimum at  $\mathbf{k}_0$ . This does not introduce divergences at the low energy range, since in this scale  $A^\zeta(\omega)$  is analytic and  $\propto \omega$  around  $\omega = 0$ .

The effect of the logarithmic singularity, and its smoothing at low energy, is that as  $\mathbf{k}_0$  is approached, the slope of  $\bar{\epsilon}^\zeta(\mathbf{k})$  increases first [compared to the almost constant slope of  $\epsilon^\zeta(\mathbf{k})$ ] and it may become infinite, resulting in a range of an S-shape triply valued and blurred band. But as  $\mathbf{k}_0$  is further approached, the slope of  $\bar{\epsilon}^\zeta(\mathbf{k})$  decreases and becomes smaller than the slope of  $\epsilon^\zeta(\mathbf{k})$  at its minimum at  $\mathbf{k}_0$ . It is likely (though we cannot prove it under the present approximations) that the slope in this minimum is zero, and that  $\bar{\epsilon}^\zeta(\mathbf{k})$  has an analytic minimum [rather than the V-shape minimum of  $\epsilon^\zeta(\mathbf{k})$ ], consistently with the fact that there is no long-range AF order. Thus  $-\bar{\epsilon}^\zeta(\mathbf{k}_0)$  presents the crossover energy from the intermediary to the low energy range. Spin-flip excitations are, largely, double-svivon absorption or emission processes. Thus,  $-2\bar{\epsilon}^\zeta(\mathbf{k}_0)$  is the energy of such an excitation at  $\mathbf{k} = \mathbf{Q}$ . This is consistent with the neutron-scattering resonance energy observed at this wave number [10]. The observation that this resonance energy is at a local maximum (for  $\mathbf{k}$  around  $\mathbf{Q}$ ) is consistent with the present result

that  $\bar{\epsilon}^{\zeta}(\mathbf{k}_0)$  is at a minimum below zero.

The optical conductivity of the doped cuprates is characterized [11] by an anomalous Drude term and a mid-IR term. The Drude term results from transitions between QE states, and (at low  $\omega$ ) also between stripon states. The mid-IR term results (at least partly) from transitions between stripon states and QE+svivon states. The mid-IR term becomes negligibly small for  $\omega \rightarrow 0$ , and one can decouple between the contributions of the QE's and stripions to conductivity for  $\omega \rightarrow 0$ .

Thus, low- $\omega$  electric current can be expressed as a sum:  $\mathbf{j} = \mathbf{j}^q + \mathbf{j}^p$ , of QE and stripon contributions (the svivons do not carry electric charge, and their effect on the current is through occupation factors). Since both the QE and the stripon states are expressed through a perturbative expansion in the auxiliary space in terms of "bare" QE and and stripon states, one can also express  $\mathbf{j} = \mathbf{j}_0^q + \mathbf{j}_0^p$ , where  $\mathbf{j}_0^q$  and  $\mathbf{j}_0^p$  are the contributions of these bare states. However, since the bare stripon states are localized, one can assume  $\mathbf{j}_0^p \cong 0$ , and thus  $\mathbf{j} \cong \mathbf{j}_0^q$  (note that  $\mathbf{j}_0^q$  and  $\mathbf{j}_0^p$  depend on the velocity distribution of the bare states, and localized states correspond to an infinite "mass" and zero velocity). Consequently one can express:

$$\mathbf{j}^q/(1-\alpha) \cong \mathbf{j}^p/\alpha \cong \mathbf{j}_0^q \cong \mathbf{j}, \quad (21)$$

where  $\alpha$  depends on expansion coefficients and occupation factors, and thus has a negligible temperature dependence.

When an electric field is applied, condition (21) is satisfied by the formation of gradients  $\nabla\mu^q$  and  $\nabla\mu^p$  of the QE and stripon chemical potentials, respectively (the treatment of the constraint provides an additional Lagrange multiplier to the electrons chemical potential). Charge neutrality imposes:

$$\frac{\partial n_e^q}{\partial \mu^q} \nabla\mu^q + \frac{\partial n_e^p}{\partial \mu^p} \nabla\mu^p = 0. \quad (22)$$

where  $n_e^q$  and  $n_e^p$  are the contributions of QE and stripon states to the electrons occupation. If one introduces:

$$N_e^q \equiv \frac{\partial n_e^q}{\partial \mu^q}, \quad M_e^p(T) \equiv T \frac{\partial n_e^p}{\partial \mu^p}, \quad (23)$$

it turns out, due to the QE and stripon bandwidths, that  $N_e^q$  is almost temperature independent, and that  $M_e^p(T)$  is temperature dependent only at low  $T$ . In the presence of an electric field  $\mathbf{E}$  one can express:

$$\mathcal{E}^q = \rho^q(T)\mathbf{j}^q, \quad \mathcal{E}^p = \rho^p(T)\mathbf{j}^p \quad (24)$$

where

$$\mathcal{E}^q = \mathbf{E} + \nabla\mu^q/e, \quad \mathcal{E}^p = \mathbf{E} + \nabla\mu^p/e, \quad (25)$$

and by Eqs. (22,23,25):

$$\mathbf{E} = \frac{M_e^p(T)\mathcal{E}^p + N_e^q\mathcal{E}^q T}{M_e^p(T) + N_e^q T}. \quad (26)$$

Since  $\mathbf{E} = \rho\mathbf{j}$ , the electrical resistivity  $\rho$  can be expressed, using Eqs. (21,24,26), as:

$$\rho = \frac{\alpha M_e^p(T)\rho^p(T) + (1-\alpha)N_e^q\rho^q(T)T}{M_e^p(T) + N_e^q T}. \quad (27)$$

This expression demonstrates that the anomalous temperature dependence of  $\rho$  is determined here by  $\rho^q(T)$ ,  $\rho^p(T)$ , and also by the temperature dependence of  $\partial n_e^p/\partial \mu^p = M_e^p(T)/T$ . Expressions will be derived below on the basis of a band model.

Eq. (21) also plays an important role in the determination of the Hall constant  $R_H = 1/en_H$ . When a magnetic field  $H = H_z$  is applied under current  $j_x$ , and an electric field  $E_y$  is required to keep  $j_y = 0$ , then the "Hall number" is:  $n_H = j_x H/eE_y$ . However, by Eq. (21) one then gets also  $j_y^q = j_y^p = 0$ , and QE and stripon "Hall effects" can be treated separately, yielding:

$$\mathcal{E}_y^q = j_x^q H/en_H^q, \quad \mathcal{E}_y^p = j_x^p H/en_H^p, \quad (28)$$

where  $n_H^q$  and  $n_H^p$  can be roughly interpreted as effective QE and stripon contributions to the density of charge carriers, and are not expected to be temperature dependent. Since (21) both  $\mathbf{j}^q$  and  $\mathbf{j}^p$  are determined by the current  $\mathbf{j}_0^q$  of the bare QE states, both  $n_H^q$  and  $n_H^p$  are expected to have same sign which corresponds to these states. By Eqs. (26,28) one can then express the Hall number as:

$$n_H = \frac{M_e^p(T) + N_e^q T}{\alpha M_e^p(T)/n_H^p + (1-\alpha)N_e^q T/n_H^q}. \quad (29)$$

Here, the anomalous temperature dependence is determined only by  $M_e^p(T)/T$ . A quantity often discussed is the Hall angle  $\theta_H$ , defined through:  $\cot\theta_H = \rho/R_H$ . By Eqs. (27,29) it is expressed as:

$$\cot\theta_H = \frac{e[\alpha M_e^p(T)\rho^p(T) + (1-\alpha)N_e^q\rho^q(T)T]}{\alpha M_e^p(T)/n_H^p + (1-\alpha)N_e^q T/n_H^q}. \quad (30)$$

When both an electric field and a temperature gradient are present, one can express  $\mathbf{j}^q$  and  $\mathbf{j}^p$  as:

$$\mathbf{j}^q = \frac{e}{T} L^{q(11)} \mathcal{E}^q + L^{q(12)} \nabla\left(\frac{1}{T}\right), \quad (31)$$

$$\mathbf{j}^p = \frac{e}{T} L^{p(11)} \mathcal{E}^p + L^{p(12)} \nabla\left(\frac{1}{T}\right). \quad (32)$$

These expressions are used to evaluate the thermo-electric power (TEP), defined as:  $S = [E/\nabla T]_{\mathbf{j}=0}$ . Since (21) the condition  $\mathbf{j} = 0$  corresponds also to  $\mathbf{j}^q = \mathbf{j}^p = 0$ , one can get by Eqs. (31,32) expressions for QE and stripon ‘‘TEP’s’’:

$$S^q(T) = \left[ \frac{\mathcal{E}^q}{\nabla T} \right]_{\mathbf{j}^q=0} = -\frac{1}{eT} \frac{L^{q(12)}}{L^{q(11)}}, \quad (33)$$

$$S^p(T) = \left[ \frac{\mathcal{E}^p}{\nabla T} \right]_{\mathbf{j}^p=0} = -\frac{1}{eT} \frac{L^{p(12)}}{L^{p(11)}}, \quad (34)$$

and through Eq. (26) express the TEP as:

$$S = \frac{M_e^p(T)S^p(T) + N_e^q S^q(T)T}{M_e^p(T) + N_e^q T}. \quad (35)$$

In order to get the temperature dependencies in the above transport expressions we need expressions for  $\tilde{A}^q(\omega)$ ,  $\tilde{A}^p(\omega)$ , and  $\tilde{A}^\zeta(\omega)$  in the low energy range [rather than the intermediary energy range expressions (10–12)]. As was mentioned above, the non-analytic behavior of the spectral functions disappears within the low energy range. For  $\tilde{A}^q$  and  $\tilde{A}^\zeta$  we assume the lowest order terms in a series expansion in  $\omega$ , thus:

$$\tilde{A}^q(\omega) \cong \text{const}, \quad \tilde{A}^\zeta(\omega) \propto \omega. \quad (36)$$

A band model of a ‘‘rectangular’’ shape of width  $\omega^p$ , and fractional occupation  $n^p$ , is assumed for  $\tilde{A}^p$ :

$$\tilde{A}^p(\omega) = \begin{cases} \frac{1}{\omega^p}, & \text{for } -\frac{\omega^p}{2} < \omega + \mu < \frac{\omega^p}{2}, \\ 0, & \text{otherwise,} \end{cases} \quad (37)$$

where  $\mu \equiv \mu^p$  (its position serves as the energy zero). Note that the inclusion of temperature dependencies in Eqs. (36,37), as well as terms of higher  $\omega$  powers in Eq. (36), would add terms of higher powers of  $T$  to the results, and thus have an effect at high-temperatures.

Since  $n^p = \int \tilde{A}^p(\omega) f_T(\omega) d\omega$ , it is straight forward to express  $\mu$  and  $M_e^p$  [we use Eq. (23), normalize the occupation numbers such that  $n_e^p = n^p$ , and express  $T$  in energy units] as:

$$\mu = T \ln \left\{ \frac{\exp[n^p \omega^p / 2T] - \exp[-n^p \omega^p / 2T]}{\exp[(1 - n^p) \omega^p / 2T] - \exp[-(1 - n^p) \omega^p / 2T]} \right\}, \quad (38)$$

$$M_e^p = (T/\omega^p) [f_T(-\frac{1}{2}\omega^p - \mu) - f_T(\frac{1}{2}\omega^p - \mu)]. \quad (39)$$

Their low and high  $T$  limits are given by:

$$\mu = \begin{cases} (n^p - \frac{1}{2})\omega^p, & \text{for } T \ll \omega^p, \\ T \ln [n^p / (1 - n^p)], & \text{for } T \gg \omega^p, \end{cases} \quad (40)$$

$$M_e^p = \begin{cases} T/\omega^p, & \text{for } T \ll \omega^p, \\ n^p(1 - n^p), & \text{for } T \gg \omega^p. \end{cases} \quad (41)$$

Expressions for  $\rho^p(T)$  and  $\rho^q(T)$  (24) are derived using linear response theory, under which  $\rho^p(T) \propto \Gamma^p(T)$  and  $\rho^q(T) \propto \Gamma^q(T)$ . Eqs. (5,6) are applied to evaluate  $\Gamma^p(\omega = 0)$  and  $\Gamma^q(\omega = 0)$ , and temperature independent terms are added to account for impurity scattering. Thus:

$$\Gamma^p \propto \int \tilde{A}^q(\omega) \tilde{A}^\zeta(\omega) [f_T(\omega) + b_T(\omega)] d\omega + \text{const}, \quad (42)$$

$$\Gamma^q \propto \int \tilde{A}^p(\omega) \tilde{A}^\zeta(\omega) [f_T(\omega) + b_T(\omega)] d\omega + \text{const}, \quad (43)$$

where the model spectral functions (36,37) are used. The result for  $\Gamma^p$  is straight forward, yielding:

$$\rho^p \cong \rho_0^p + \rho_2^p T^2. \quad (44)$$

The integral (43) for  $\Gamma^q$  does not have a rigorous analytical result, however an approximate one can be derived based on the two leading terms in a high- $T$  expansion, joined smoothly with an approximate low- $T$  limit term. It can be expressed as:

$$\rho^q \cong \rho_0^q + \rho_1^q \begin{cases} AT - \frac{B}{T}, & \text{for } T > \sqrt{\frac{2B}{A}}, \\ \frac{A}{2} \sqrt{\frac{A}{2B}} T^2, & \text{for } T < \sqrt{\frac{2B}{A}}, \end{cases} \quad (45)$$

where the positive constants  $A$  and  $B$  are expressed in terms of the above stripon band parameters.

The stripions contribution to the TEP is derived here through [12]:

$$S^p \cong -\frac{k_B}{e} \frac{\int \tilde{A}^p(\omega) \frac{\omega}{T} \frac{df_T(\omega)}{d\omega} d\omega}{\int \tilde{A}^p(\omega) \frac{df_T(\omega)}{d\omega} d\omega}, \quad (46)$$

where  $k_B$  is Boltzmann’s constant ( $k_B/e = 86 \mu\text{V/K}$ ). Inserting (37) in (46), and using (38,39), one gets:

$$S^p \cong \frac{k_B}{eM_e^p} \left\{ \frac{1}{2} [f_T(-\frac{1}{2}\omega^p - \mu) + f_T(\frac{1}{2}\omega^p - \mu)] + \frac{\mu M_e^p}{T} - n^p \right\}, \quad (47)$$

with low and high  $T$  limits:

$$S^p \cong \frac{k_B}{e} \begin{cases} 0, & \text{for } T \ll \omega^p, \\ \ln [n^p / (1 - n^p)], & \text{for } T \gg \omega^p. \end{cases} \quad (48)$$

In order to apply an expression similar to Eq. (46) to derive  $S^q$  (replacing  $\tilde{A}^p$  there by  $\tilde{A}^q$ ), a linear term  $a^q \omega$  should be added to  $\tilde{A}^q(\omega)$  in Eq. (36), resulting in a metallic linear  $T$  behavior:

$$S^q \cong S_1^q T, \quad (49)$$

where the constant  $S_1^q$  has an opposite sign than  $a^q$ . The inequalities (19), and the smoothening of the

discontinuity in  $\tilde{A}^q(\omega)$  in the low energy range, results in  $a^q > 0$ , and thus  $S_1^q < 0$  for p-type cuprates [for which (19) is valid] while [following the discussion after Eq. (19)] for “real” n-type cuprates  $a^q < 0$ , and thus  $S_1^q > 0$ .

The transport coefficients are calculated using Eqs. (27,29,30,35,38,39,44,45,47,49) for five stoichiometries, ranging from underdoped ( $n^p = 0.8$ ) to overdoped ( $n^p = 0.4$ ) p-type cuprates.  $N_e^q$  is assumed to increase with doping, reflecting transfer of QE spectral weight towards  $E_F$ . Consequently (6)  $\omega^p$  is assumed to decrease with doping. We introduce  $\tilde{n}_H^p \equiv n_H^p/\alpha$  and  $\tilde{n}_H^q \equiv n_H^q/(1-\alpha)$ , and they are assumed to increase with doping, where  $\tilde{n}_H^p$  increases considerably faster than  $\tilde{n}_H^q$ , and a little faster than  $1-n^p$  (since  $\tilde{n}_H^p$  reflects an overall stripon-related carriers density, while  $n^p$  is the fractional occupation of stripon states within the charged stripes whose number increases with doping). In order to separate the effect of doping on the density of states and the carriers density we introduce  $\tilde{\rho}_0^p \equiv \rho_0^p n_H^p/N_e^q$ ,  $\tilde{\rho}_2^p \equiv \rho_2^p n_H^p/N_e^q$ ,  $\tilde{\rho}_0^q \equiv \rho_0^q n_H^q(1-n^p)/n_H^p$ , and  $\tilde{\rho}_1^q \equiv \rho_1^q n_H^q(1-n^p)/n_H^p$ , and assume doping-independent values of  $\tilde{\rho}_0^p$ ,  $\tilde{\rho}_2^p$ ,  $\tilde{\rho}_0^q$ , and  $\tilde{\rho}_1^q$ . Results for a specific choice of the parameters are presented in Fig. 1. These results, however, do not include the effect of the pseudogap.

The results for  $S$  [Fig. 1(a)] reproduce very well the systematic TEP behavior, which is characteristic of the doping level [13–15] (determined here mainly through  $n^p$ ). The position of the maximum in  $S$  depends on the choice of  $\omega^p$ . This maximum may be below or above  $T_c$ , and the occurrence of a pseudogap may shift it to a higher temperature than predicted here. Electron bands which are not coupled to the stripions in the  $\text{CuO}_2$  planes may have a linear contribution to  $S$  deviating from our prediction. Also the results for  $n_H$  and  $R_H$  [Fig. 1(b,c)] reproduce very well the systematic Hall behavior [16,17]. The increasing linear  $T$  dependence of  $n_H$  reflects a crossover from, approximately, the smaller  $\tilde{n}_H^p$  at low  $T$  to the larger  $\tilde{n}_H^q$  at high  $T$ . The results for  $\rho$  and  $\cot\theta_H$  [Fig. 1(d,e)] reproduce very well the systematic experimental behavior too [16,17]. An approximate quadratic  $T$  dependence of  $\cot\theta_H$  is obtained in the temperature range where  $n_H$  is linear in  $T$ . The linear  $T$  behavior of  $\rho$  persists through the high-temperature saturation range of  $R_H$  [17]. Cases of non-quadratic  $T$  dependence of  $\rho$  at very low  $T$  are expected as a pseudogap effect.

In “real” n-type cuprates  $S$  is expected to behave similarly to p-type cuprates, for similar doping levels, but with an opposite sign (and slope). TEP results for NCCO [18] show that in superconducting doping levels it has the same behavior as in p-type

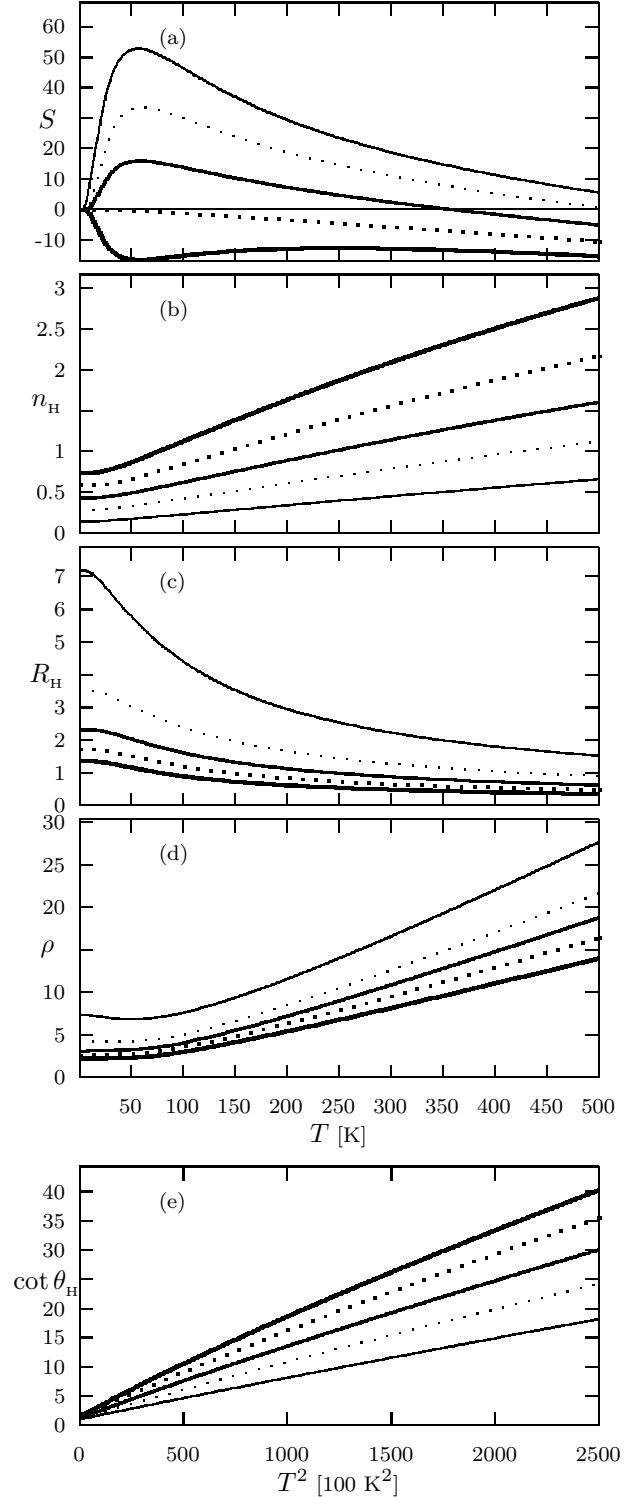


FIG. 1. The transport coefficients, in arbitrary units [and  $\mu\text{V}/\text{K}$  units for  $S$  (a)], for:  $n^p=0.8,0.7,0.6,0.5,0.4$ ;  $10000N_e^q=20,23,26,29,32$ ;  $\omega^p[\text{K}]=200,190,180,170,160$ ;  $\tilde{n}_H^p=0.1,0.2,0.3,0.4,0.5$ ;  $\tilde{n}_H^q=6,7,8,9,10$ ;  $S_1^q=-0.025$ ;  $\tilde{\rho}_0^p=500$ ;  $\tilde{\rho}_2^p=0.03$ ;  $\tilde{\rho}_0^q=5$ ;  $\tilde{\rho}_1^q=0.2$ . The last values correspond to the thickest lines.

cuprates [Fig. 1(a)], but with an opposite effect of doping. Namely  $S$  for lower doping levels is typical of the p-type overdoped regime. This indicates that NCCO is probably not a “real” n-type cuprate, and its stripons are also based on holon states, where the extra doped negative charge occupies another QE band. The Hall constant in NCCO [18] is consistent with Fig. 1(d), and our prediction that the sign of both  $n_H^p$  and  $n_H^q$  is determined by the bare QE states (and changes in NCCO with doping).

The coupling Hamiltonian  $\mathcal{H}'$  (4) provides a mechanism for high- $T_c$ . The pairing is introduced by transitions between pair states of stripons and QE’s through the exchange of svivons [5]. Such transitions enable long-range hopping of local stripon pairs, without an associated hopping of svivons (necessary for single-stripon hopping). Thus the pairing results in a large gain in the “kinetic” energy of the stripons, which can effectively be expressed as a strong attractive stripon-stripon interaction.

Pair-breaking is expected here to result in QE and stripon+svivon excitations. ARPES measurements in the superconducting state [19] show a sharp peak at  $\sim 0.04$  eV over a wide range of the BZ, and a “hump” starting at  $\sim 0.1$  eV and merging with a normal-state band at higher energies. The hump is consistent with a QE pair-breaking excitation, and the peak is consistent with a stripon+svivon pair-breaking excitation at the svivon minimum excitation energy  $-\tilde{\epsilon}^s(\mathbf{k}_0)$ . In the superconducting state this minimum is within the gap, resulting in a considerably narrower level than in the normal state [reflected also in the neutron-scattering resonance energy  $-2\tilde{\epsilon}^s(\mathbf{k}_0)$ ]. This results in a sharp pair-breaking excitation peak over a wide range of the BZ, due to the flatness of the stripon band.

It has been suggested [20] that the cuprates fall in the regime of crossover between BCS and preformed-pairs Bose-Einstein condensation (BEC) behaviors. Such a crossover occurs if the pairing energy becomes as large as the relevant bandwidth, and this condition is fulfilled here due to the small stripon bandwidth. The BEC behavior occurs in the underdoped cuprates, where singlet pairs are formed at  $T_{\text{pair}}$ , and superconductivity occurs below  $T_{\text{coh}} (< T_{\text{pair}})$  where phase coherence sets in.

The pseudogap is then a pair-breaking gap between  $T_{\text{coh}}$  and  $T_{\text{pair}}$ ; it has similarities to the superconducting gap, and accounts for most of the pairing energy. The coherence temperature can be expressed [21] as:  $T_{\text{coh}} \propto n_s/m_s^*$ , where  $m_s^*$  is the pairs effective mass and  $n_s$  is their density, in agreement with the “Uemura plots” [22]. Our observation [Fig. 1(a)] that the stripon band is half full

( $n^p = \frac{1}{2}$ ) for slightly overdoped cuprates results in the “boomerang-type” behavior [23] of the Uemura plots in overdoped cuprates. It is due to a crossover between a stripon band-top  $T_c = T_{\text{coh}}$  behavior in the underdoped cuprates, and a stripon band-bottom  $T_c = T_{\text{pair}}$  behavior in overdoped cuprates.

In conclusion, it was demonstrated here that a realistic treatment of the cuprates, taking into account the effects of both large- $U$  and small- $U$  orbitals, and of the inhomogeneities introduced by a dynamical striped structure, resolves puzzling normal-state spectroscopic and transport properties, and provides a mechanism for high- $T_c$  superconductivity and the occurrence of a normal-state pseudogap.

## REFERENCES

1. S. E. Barnes, *Adv. Phys.* **30**, 801 (1980).
2. J. Ashkenazi, *J. Supercond.* **7**, 719 (1994).
3. V. J. Emery, and S. A. Kivelson, *Physica C* **209**, 597 (1993).
4. Papers in *Int. J. Mod. Phys.* **14**, 3289–3790 (2000).
5. J. Ashkenazi, *High-Temperature Superconductivity*, edited by S. E. Barnes, J. Ashkenazi, J. L. Cohn, and F. Zuo (AIP Conference Proceedings 483, 1999), p. 12; cond-mat/9905172.
6. A. Bianconi, *et al.*, *Phys. Rev. B* **54**, 12018 (1996).
7. H. Eskes, *et al.*, *Phys. Rev. Lett.* **67**, 1035 (1991).
8. Z. X. Shen, *et al.*, cond-mat/0108381; this issue.
9. P. D. Johnson, *et al.*, *Phys. Rev. Lett.* **87**, 177007 (2001).
10. H. F. Fong, *et al.*, *Phys. Rev. B* **61**, 14773 (2000).
11. D. B. Tanner, and T. Timusk, *Physical Properties of High Temperature Superconductors III*, edited by D. M. Ginsberg (World Scientific, 1992), p. 363.
12. S. Bar-Ad, B. Fisher, J. Ashkenazi and J. Genossar, *Physica C* **156**, 741 (1988).
13. B. Fisher, *et al.*, *J. Supercond.* **1**, 53 (1988); J. Genossar, *et al.*, *Physica C* **157**, 320 (1989).
14. S. Tanaka, *et al.*, *J. Phys. Soc. Japan* **61**, 1271 (1992).
15. K. Matsuura, *et al.*, *Phys. Rev. B* **46**, 11923 (1992); S. D. Obertelli, *et al.*, *ibid.*, p. 14928; C. K. Subramaniam, *et al.*, *Physica C* **203**, 298 (1992).
16. Y. Kubo and T. Manako, *Physica C* **197**, 378 (1992).
17. H. Takagi, *et al.*, *Phys. Rev. Lett.* **69**, 2975 (1992); H. Y. Hwang, *et al.*, *ibid.* **72**, 2636 (1994).
18. J. Takeda, *et al.*, *Physica C* **231**, 293 (1994); X.-Q. Xu, *et al.*, *Phys. Rev. B* **45**, 7356 (1992); Wu Jiang, *et al.*, *Phys. Rev. Lett.* **73**, 1291 (1994).
19. M. R. Norman, and H. Ding, *Phys. Rev. B* **57**, R11089 (1998).
20. M. Randeria, cond-mat/9710223, Varenna Lectures (1997); J. R. Engelbrecht, *et al.*, *Phys. Rev. B* **55**, 15153 (1997); R. D. Duncan, and C. A. R. Sá de Melo, *ibid* **62**, 9675 (2000); Q. Chen, *et al.*, *ibid* **63**, 184159 (2001).
21. V. J. Emery, and S. A. Kivelson, *Nature* **374**, 4347 (1995).
22. Y. J. Uemura, *et al.*, *Phys. Rev. Lett.* **62**, 2317 (1989).
23. Ch. Niedermayer, *et al.*, *Phys. Rev. Lett.* **71**, 1764 (1993).